Relative Misalignments Estimation in On-tracker CPV Modules through Image Processing

Luis San José[1, a)] Rebeca Herrero[1] and Ignacio Antón[1]

https://orcid.org/0000-0002-6869-0613
https://orcid.org/0000-0003-4309-6084
https://orcid.org/0000-0002-6890-5477
[1]*Institute of Solar Energy, Universidad Politécnica de Madrid, Avda/Complutense 30, 28040, Madrid, Spain*
[a)]luis.sanjose@ies.upm.es

Abstract. This work uses a validated method to measure misalignments between optic units in CPV modules indoors (using a camera) to measure misalignments between modules outdoors. Since the measurement outdoors has different condition than indoors, acquired images require an enhancement, reached through image processing. A case study for 3 modules with known misalignments is presented for the method validation.

INTRODUCTION

Concentrator Photovoltaic (CPV) is a technology that uses optical systems to focus sunlight into small high-efficient solar cells [1]. These optical systems are usually compound of a lens as Primary Optic Element (POE) and another secondary optical element (SOE) coupled to the photovoltaic solar cell that can be reflective or refractive.

The angular acceptance of a concentrator describes the maximum deviation angle of the incident light beam (with respect to the normal of the optical system) that is concentrated (i.e., transmitted form the input aperture area to the output aperture area of the concentrator). The maximum achievable angular acceptance α_{max} for a given optical design is inversely linked to the geometrical concentrator factor as given by the conservation of Étendue [2], it can vary through its input aperture area, and also can be defined positive or negative with respect to the normal of the optical system, thus $+\alpha_{max}$ or $-\alpha_{max}$ may be used. Incident light with α_{max} is concentrated into the receiver edges.

The 1-dimensional angular transmittance $H(\alpha)$ function of a concentrator describes the percentage of light beams with an incident angle α that, illuminating uniformly (along one single axis) the input aperture area of the concentrator, are focused at its output. The function can be derived from the angular acceptance variation along the aperture. In this study, the shape of the angular transmittance is approximated to a box function, which implies that the lens has the same angular acceptance α_{max} over its aperture (Fig.1.a).

Because the narrow angular acceptance of a concentrator (typically below 1 degree), a CPV system performance depends on the correct optical alignment among sub-parts. Consider the case of a concentrator formed by a Fresnel lens and a receiver (photovoltaic cell) at its focus, and the same concentrator but with the receiver displaced slightly from its optimum (in the same plane parallel to the Fresnel lens). If we compare the two angular transmittance functions (with and without receiver displacement) for a given concentrator, both angular transmittances are equals but with an angular offset (Fig.1.a). This offset value is what we called misalignment φ, which represents the difference between the α_{max} in both functions, and as stated before, α_{max} is linked with the receiver edges.

An observer in front of the concentrator under study see the receiver magnified by the Fresnel lens. For the case in which the receiver is misaligned, the image formed through the lens is not perfectly centered, but displaced with respect to the optics aperture. Thus, if the edges (which are linked to α_{max}) of the receivers through several lenses are compared, the displacement of the receivers can be gathered. Translating these displacements in millimeters to angles, misalignments between units can be obtained. Notice that, although the receiver displacement is causing the

misalignment in this example, other mechanical errors may cause misalignments between units in a module, such as the attaching and alignment of the parquet of POEs to the module chassis or the SOE attaching to the receiver. These misalignments between units determine the optimum pointing vector of the module with respect to the sun. Therefore, misalignments can also be evaluated at tracker level, in which differences in the pointing vector of modules may reduce the system output.

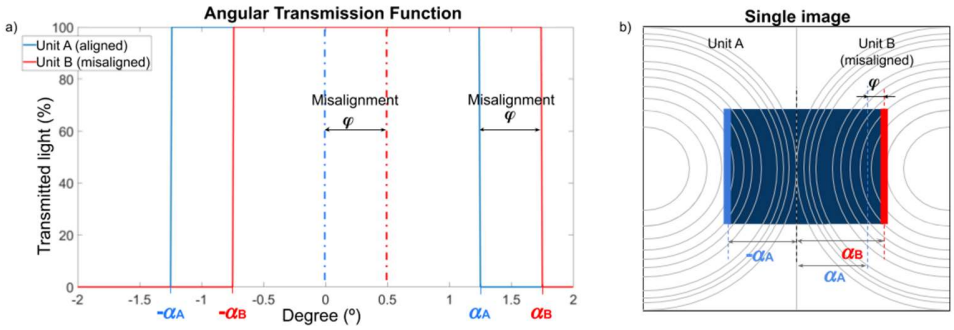

FIGURE 1. (a) Angular transmission function (box-shaped) for two units, one of which presents a misalignment. (b) Scheme that represents an intersection of the two units where, for each unit, lens forms the corresponding image of the receiver.

This paper presents a measurement method to obtain misalignments that substitutes the observer by a camera that photographs the receiver through the lens. Moreover, instead of taking one image per unit (i.e. to observe one receiver through its lens), the image is taken in an intersection between units to obtain differences between the receivers' edges (Fig.1.b), which are translated to relative misalignments between the units. To improve the quality of the images and thus to reduce the uncertainty in the receiver edges recognition, an image processing must be performed. A case study, in which misalignments between modules are measured, is presented, explaining deeply the needed image processing.

PREVIOUS WORK & MOTIVATION

In previous works [3], misalignments between lens-receiver units of a module were measured through this image acquisition method by comparing the receivers' areas seen through the optical system of the concentrator (Fig.2.a shows an example of used images). The method was validated against a system called the Module Optical Analyzer (MOA) [4]. The MOA is based on the Luminescence Inverse method [5], that measures (by using a large collimator mirror) the pseudo Lambertian light emitted by the cells (when module is forward biased) to obtain the angular properties of all module units. The method has some advantages compared with MOA: there is no need of forward bias the module, nor using a collimator as large as the module area, and it is suitable to be used outdoors.

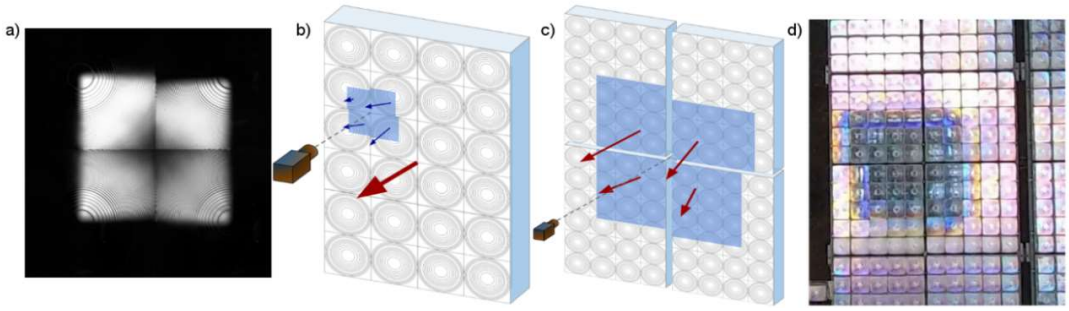

FIGURE 2. (a) Image taken in an intersection of units: 4 receivers are seen through their corresponding lenses. (b) Scheme of the misalignments measurement between units (the camera is placed near the module). (c) Scheme of the misalignments measurement between modules (camera at large distance from module). (d) Image taken at an intersection of modules.

Varying the distance between the camera and the CPV part, the method is able to determine both intra-module misalignments at the production line and outdoors on-tracker module misalignments on a CPV system (see schemes in Fig.2.b and Fig.2.c). For this last case, an image is taken in the intersection of modules (Fig.2.d).

The aim of this presented work is to apply the proposed method to measure misalignments between modules. In the next paragraph, a case study is presented, where misalignments between three modules installed on a tracker have been measured. After this, an image processing that allows identifying the size of the receivers seen through the optics is presented. The measured misalignments are compared with the real values in order to validate the method outdoors and analyze the adequacy of the image processing.

CASE OF STUDY

Three identical FLATCON modules with a concentration ratio 500x composed by 200 cells without SOE and a POE formed by 4cm-squared Fresnel lenses have been placed on a tracker, introducing known misalignments between them. From now on, these known misalignments are referred as real values in the paper. To apply the method, the camera is placed at a sufficient distance to distinguish the receiver image area through several lenses. For this case, only two images at the modules intersections are needed (Fig.3.a). To obtain relative misalignments, the same reference must be used for all the images taken, in this case, the misalignment of central module.
Because the observed magnified receivers' areas can be associated to the angular acceptance α_{max}, differences in their positions inform about misalignments between the modules. Once the receiver edges with rhomb shape are determined, the differences between the upper (α_1 and α_2 in Fig.3.a) or lower ($-\alpha_2$ and $-\alpha_3$) vertexes are considered.

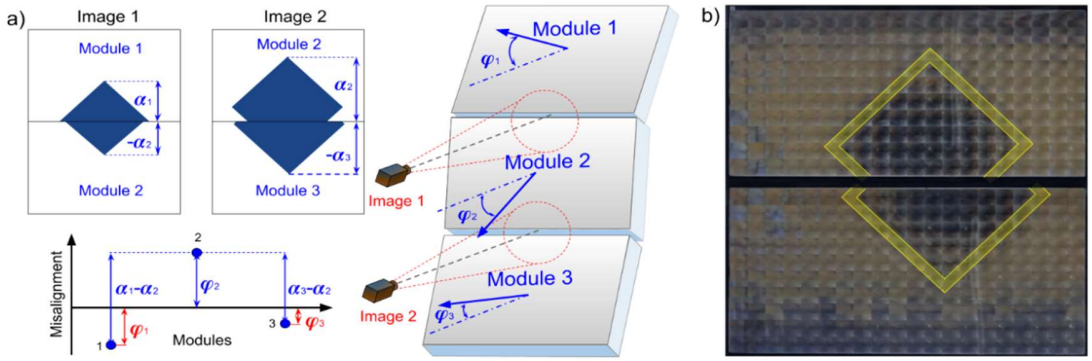

FIGURE 3. (a) Representation of the images to be obtained and the distances to the vertexes that have to be determined (left). Representation of the measurement set up (right). (b) Example of an image acquired in an intersection between modules.

The obtained module images present important problems to define the receivers' areas seen through the lenses parquet (Fig.3.b). First, the contrast between the receiver area and the rest of the module backsheet seen through the lenses is low. Second, the area of the receiver image presents bright spots, due to reflections in the lenses parquet. Thus, the edges of the receiver image result diffuse.

An adequate image processing is required to enhance the contrast between receiver area and the rest of the module as much as possible, to avoid bright spots (and homogenize areas) and to perform a thresholding that recognizes edges on the same bases independent on the photograph's quality. Next paragraph gives a detailed explanation of the image processing applied to enhance the images is, which seeks to reduce the uncertainty associated to the receiver area definition and to increase the accuracy of the measured misalignments between modules.

PROCESSING

As presented in the previous section, differences between the vertexes of the receivers seen through the POE are proportional to the misalignments between the units under test. However, the images of the receivers formed at infinity by the POEs are somewhat blurred (see Fig.3.b) and an image processing is needed to reduce the uncertainty in the area definition (yellow area in images of Fig.4). The developed image processing (performed in MATLAB) has two main objectives: to increase the contrast between the dark areas (e.g. the receiver seen through the lenses) and the other light areas (e.g. the backsheet of the module), and to homogenize each of these two different kind of areas (by reducing bright spots at the POE). The proposed algorithm comprises several steps (as shown in Fig.4) that are explained in the following paragraphs.

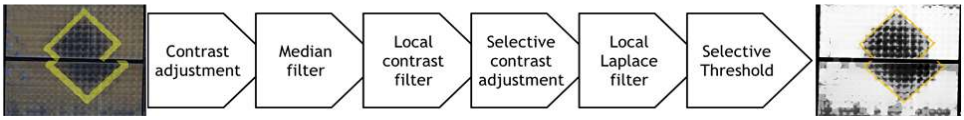

FIGURE 4. Steps of the developed image processing algorithm

The first step in the image processing is to highlight colors to make the different areas more noticeable. Thus, a histogram contrast adjustment is applied in each of the RGB channels of the image separately. Fig.5.a shows the image before (upper) and after (lower) this adjustment, together with their histograms. This consists on extending the histogram until 1% of its values are white and 1% black. After this step, the receiver area darkens and the rest of the area has lighter colors. However, bright spots are also enhanced. A median filter (that uses a mask or kernel to obtain the mean value of each pixel and its eight immediate neighbors) is used to reduce bright spots. This filter also produces a light blur. Fig.5.b shows a detail of the image before (upper) and after (lower) the median filter.

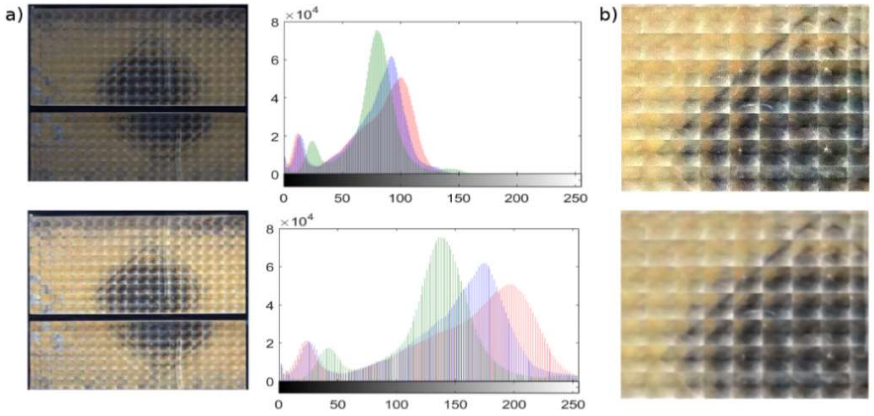

FIGURE 5. (a, upper) Original image and its histogram for the RGB channels. (a, down) Image and histogram after contrast adjustment. (b, upper) Image detail after contrast adjustment. (b, down) Image detail after contrast adjustment and median filter.

Third step is a local contrast adjustment. This filter enhances the contrast only between high-contrasted regions without altering the edges, enhancing the two kind of areas (e.g., receiver and backsheet) thanks to its local performing. This filter, first detects color transitions by creating a mask, which is product of subtracting from the original image a blurred copy. This mask, along with a high-contrasted copy and the original image, maps larger-scale transitions than the edges mapped when sharpening an image. Thus, the parameters that must be adjusted are the unaltered strong edges amplitude, (that is, the minimum color step to consider an edge), and the amount of desired enhancement, (that is, level of detail in the contrasted regions). After several tests with different parameters, the edges amplitude (that ranges from 0 to 1) has been set to its maximum (due to the importance that receiver edges have). The amount of enhancement (range [-1, 1]) if is set under zero causes a smoothing of the regions, whereas if it is positive, it sharpens the contrast details. Because the intention is to obtain large homogeneous contrasted areas this value was set to 0.2. The result of this filter is shown in Fig.6.

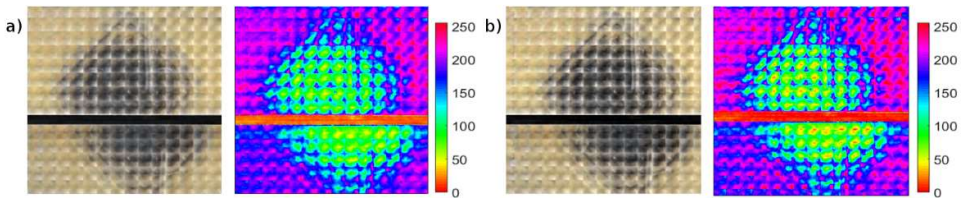

FIGURE 6. Image and color representation before the local contrast adjustment (a) and after the local contrast adjustment (b).

Despite the moderate enhancement value chosen for the local contrast adjustment, the image colors range increases. To avoid this unwanted effect (and homogenize areas), next step is a selective increase of brightness. This implies a contrast adjustment for pixels over a brightness value given, that are converted to clear values (Fig.7.b).

When a better-defined dark area through these four steps is achieved, a Laplacian local filter helps to obtain an image where edges are preserved, details enhanced and tones are homogenized. (Fig.7.c). As Gaussian pyramid based filters avoid halos in images computing scaling factors to the image gradients [6,7], this filter uses Laplacian pyramids, that apply derivative recursive filters in which parameters such as the threshold of the intensity variation, the shape of the Laplacian step and the shape of the tone-mapping curve have to be fixed previously. The threshold of the intensity variation (σ) is the minimum step in the Laplacian domain to consider an edge, the range of this scalar parameter goes from 0 to 1. Because the preservation of edges is a key feature in the processing, it was fixed to 0.25. On the other hand, the shape of the Laplacian step controls the smoothing of details (α); in other words, it controls the shape of the point-wise function for the contrast manipulation. This parameter ranges from 0.01 to 10; if it is less than 1, it increases the details and enhances local contrast, if it is greater than 1, it smooths the details, preserving the encountered edges. Enhancing the details will raise the bright spots and the inhomogeneities in the image, therefore α was fixed to 5 in order to perform an areas smoothing. Last parameter is the shape of the tone-mapping curve (β), which controls the intensity range in the image and ranges from 0 to 5. The tone-mapping curve shape determines if similar tones are merged or splitted (i.e. the dynamic range of the image is extended). Because α smooths the image, if β is fixed to a value that expands the dynamic range in the image, the contrast will be enhanced too in the image without causing inhomogeneities in similar color areas, therefore, β was fixed to 3.

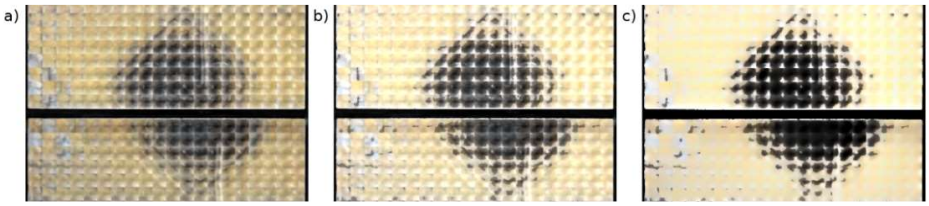

FIGURE 7. Image after local contrast adjustment (a), after selective contrast adjustment (b) and after Laplacian local filter (c).

After this, a binarization of the image can be performed to obtain a mask that added to the original image gives a clearer and more homogeneous definition of the receiver area. In order to choose an adequate threshold level, a multithresholding is applied at 2 and 5 levels. A multithresholding finds N threshold values using Otsu's method [8] and quantifies the image into N+1 regions. The resulting image from a 2 (N) levels multithresholding is divided in 3 (N+1) regions, as shown in Fig.8.a. Whereas this 3 region segmentation (N=2) helps to distinguish the bright areas, the 6 region segmentation (N=5) helps to refine the dark receiver area, as shown in Fig.8.b. Using both multi-threshold images, a single binarized image in two levels is obtained (taking the 2 and the 4 darker regions in the 3-regions and 6-regions image respectively as 0). The resulting image can be used as a mask to enhance the original image, sharpening the receiver edges. Before that, morphological operations are applied to refine the receiver area, without altering the receiver edges, using a symmetrical structure element (Fig.8.c). An opening erases little white areas and smooth irregular edges, and then, a closing merges big white areas and uniforms them. Finally, the obtained mask is added to the original image, resulting an image where the receiver area seen through the module lenses is well defined and the edges are preserved and enhanced during these steps (Fig.8.d).

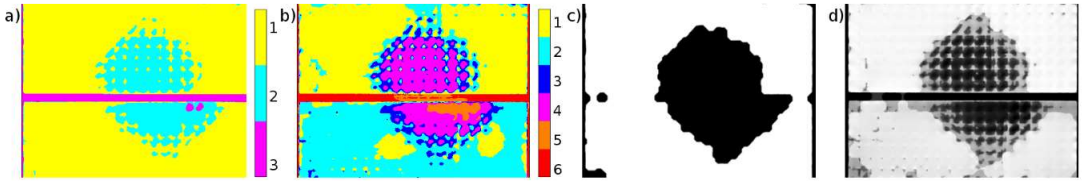

FIGURE 8. (a)image with a 3 region thresholding (N=2) (b) image with a 6 region thresholding (c) mask or image after binarization (d) Image after the addition of the mask to the original image.

RESULTS

In Fig.9 measured misalignments for two sets of images taken at two different distances (camera-module) are shown. For each set, differences in the vertexes position of the receivers have been measured, and its associated misalignments have been calculated. For each image, the vertexes positions have been determined three times in order to obtain an averaged misalignment measure. The measurement error is defined as the mean of the differences (in

percentage) between the measured misalignment in each of the two images and the real value (considering the two distances). The uncertainty associated to the measurement is defined as the difference between the minimum and the maximum misalignment value measured for each of the modules due to the blurring in the edges definition. When receivers' areas in the images have been measured without processing, determining its edges resulted difficult, which made measurements to present errors above 50%. Depending on the criteria taken to define edges, results were quite variable too, making the uncertainty unacceptable (±0.37º). With the same sets of images, due to the receiver area sharpening reached with the processing, a more accurate measurement is obtained, with errors lower than 9% (0.04º). Because is easier to spot the receiver area in these images, the measurement repeatability improves too (reducing the uncertainty to ±0.09º). Thus, the uncertainty is lower and obtained values are closed to the real ones when both images sets are processed, which validates not only the method, but the developed processing. The real misalignment has an uncertainty of 0.1º associated to the instrumentation used to measure the modules deviation from the tracker structure.

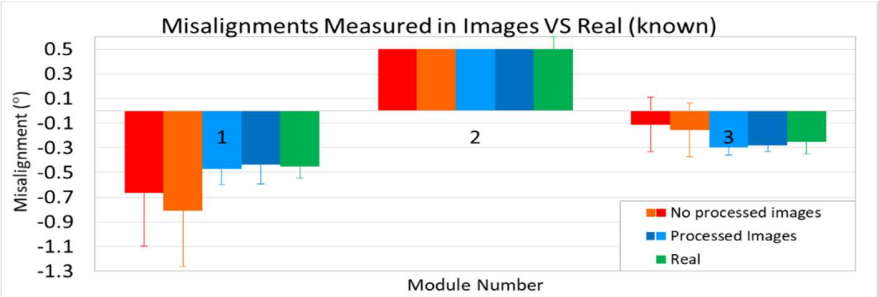

FIGURE 9. Comparison of misalignments measured using non-processed and processed images against the real value. The pairs red-clear blue and orange-dark blue correspond to images taken at a same camera-module distance respectively.

CONCLUSIONS AND FUTURE WORK

A very simple method for relative misalignments estimation in on-tracker modules has been validated. It has been checked out that the outdoors method reliance depends strongly on the processing applied to the images, which contributes to improve accuracy and to reduce uncertainty. The method will be applied to drone inspection in CPV plants to measure more quickly and effectively.

ACKNOWLEDGEMENTS

This work has been supported by the Comunidad de Madrid Program MADRID-PV2 P2018/EMT-4308, with co-funding from Fondo Europeo de Desarrollo Regional (FEDER) and Fondo Social Europeo (FSE)-Unión Europea and by the Spanish Ministerio de Economía y Competitividad (MINECO) under the program RETO (RTC-2015-3982-3).

REFERENCES

1. M. Wiesenfarth, I. Anton, and A. W. Bett, 'Challenges in the design of concentrator photovoltaic (CPV) modules to achieve highest efficiencies', (2018) *Applied Physics Reviews*, vol. 5, no. 4, p. 041601.
2. R. Winston, J. C. Miñano, and P. G. Benitez, (2005). "Nonimaging optics". Elsevier.
3. L. San José, R. Herrero, I. Antón, G. Sala, "Computer vision algorithm for relative misalignments estimation in CPV modules", (2018) *AIP Conference Proceedings*, (2012), art. no. 100004.
4. R. Herrero *et al.*, 'Experimental analysis and simulation of a production line for CPV modules: impact of defects, misalignments, and binning of receivers', (2017), *Energy Science & Engineering*, vol. 5, no. 5, pp. 257–269.
5. R. Herrero, C. Domínguez, S. Askins, I Antón, ang G. Sala, "Luminescence inverse method for CPV optical characterization", (2013) *Optics Express*, 21 (106), pp. A1028-A1034.
6. S. Paris, S. W. Hasinoff, J. Kautz, "Local Laplacian filters: Edge-aware image processing with a Laplacian pyramid" (2015) *Communications of the ACM*, 58 (3), pp. 81-91.
7. M. Aubry, S. Paris, S. W. Hasinoff, J. Kautz, F. Durand, "Fast local Laplacian filters: Theory and applications" (2014) *ACM Transactions on Graphics*, 33 (5), art. no. 167.
8. N. Otsu, "A threshold selection method from gray-level histograms", (1979) *IEEE transactions on systems, man, and cybernetics*, 9(1), 62-66.